BIOCHEMISTRY

 Volume 43, Number 47 November 30, 2004

Articles

Crystal Structure of the PH−BEACH Domains of Human LRBA/BGL†

Damara Gebauer,‡,§ Jiang Li,‡,§ Gerwald Jogl,‡ Yang Shen,‡ David G. Myszka,|| and Liang Tong*,‡

Department of Biological Sciences, Columbia University, New York, New York 10027, and Center for Biomolecular Interaction Analysis, University of Utah, School of Medicine, Salt Lake City, Utah 84132

Received March 12, 2004; Revised Manuscript Received August 21, 2004

ABSTRACT: The beige and Chediak−Higashi syndrome (BEACH) domain defines a large family of eukaryotic proteins that have diverse cellular functions in vesicle trafficking, membrane dynamics, and receptor signaling. The domain is the only module that is highly conserved among all of these proteins, but the exact functions of this domain and the molecular basis for its actions are currently unknown. Our previous studies showed that the BEACH domain is preceded by a novel, weakly conserved pleckstrin homology (PH) domain. We report here the crystal structure at 2.4 Å resolution of the PH−BEACH domain of human LRBA/BGL. The PH domain has the same backbone fold as canonical PH domains, despite sharing no sequence homology with them. However, our binding assays demonstrate that the PH domain in the BEACH proteins cannot bind phospholipids. The BEACH domain contains a core of several partially extended peptide segments that is flanked by helices on both sides. The structure suggests intimate association between the PH and the BEACH domains, and surface plasmon resonance studies confirm that the two domains of the protein FAN have high affinity for each other, with a K_d of 120 nM.

The beige and Chediak−Higashi syndrome (BEACH)[1] domain is a module of about 300 amino acid residues that is highly conserved in a large family of eukaryotic proteins (*1*). The name BEACH is derived from *beige* and Chediak-Higashi syndrome (CHS). CHS is a rare, autosomal recessive disorder that can cause severe immunodeficiency and albinism in humans and other mammals, and *beige* is the name for the CHS disease in mice (*2*−*4*). The CHS disease is associated with the presence of giant, perinuclear vesicles (lysosomes, melanosomes, and others) in many cells of the patients (*2*, *5*), and therefore, the CHS protein may have an important role in the fusion, fission, or trafficking of these vesicles.

Genomes of higher eukaryotes encode more than one BEACH proteins. The human genome may contain 8 such proteins, including CHS (*6*−*8*), neurobeachin (Nbea) (*9*), LRBA (also known as BGL, beige-like, or CDC4L) (*10*, *11*), FAN (*12*, *13*), and KIAA1607 (*14*). In the slime mold *Dictyostelium*, there are 6 BEACH proteins, LvsA−LvsF (*1*, *15*, *16*).

Most of the BEACH proteins are very large, with more than 2000 amino acid residues. Human CHS protein, with 3801 residues (Figure 1A), is among the largest BEACH proteins identified so far. FAN is the smallest BEACH protein, but it still has about 900 residues (Figure 1A). The sequence homology among these proteins is limited to their

† This research is supported in part by a Grant (GM066753 to L.T.) from the National Institutes of Health.

* To whom correspondence should be addressed. Phone: (212) 854-5203. Fax: (212) 854-5207. E-mail: tong@como.bio.columbia.edu.

‡ Columbia University.

§ These authors contributed equally to this work.

|| University of Utah, School of Medicine.

[1] Abbreviations: AKAP, A kinase-anchoring protein; BEACH, beige and Chediak−Higashi syndrome; CHS, Chediak−Higashi syndrome; LPS, lipopolysaccharide; Nbea, neurobeachin; NCS, noncrystallographic symmetry; PH, pleckstrin homology.

10.1021/bi049498y CCC: $27.50
Published on Web 11/03/2004

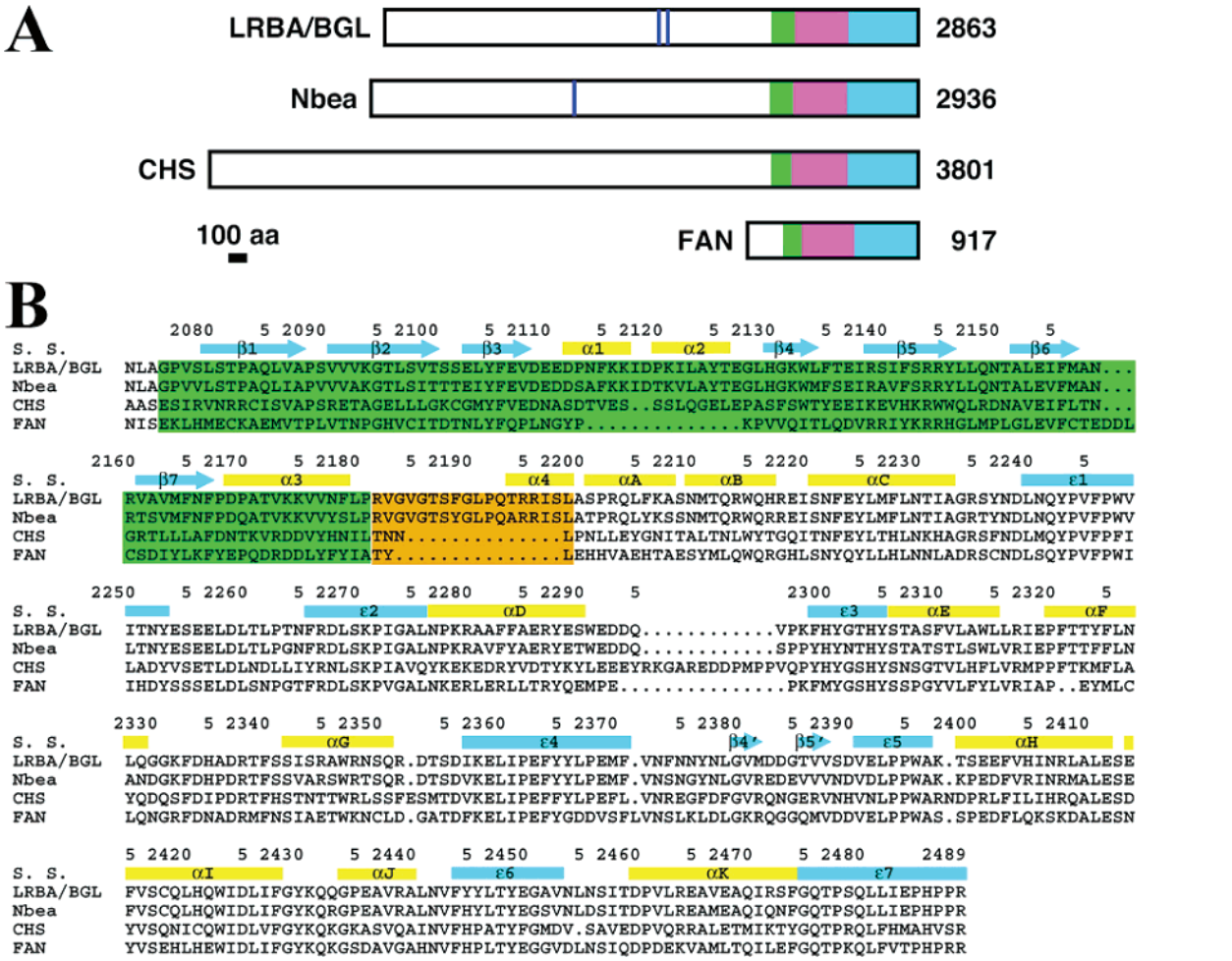

FIGURE 1: Primary structures of the BEACH proteins. (A) Schematic drawing of the primary structures of LRBA/BGL, Nbea, CHS, and FAN. The PH, BEACH, and WD40 domains are shown in green, purple, and cyan, respectively. The blue bars in LRBA/BGL and Nbea indicate the AKAP motif. (B) Alignment of the PH and BEACH domain sequences. The PH domain and the linker are shown with a green and gold background, respectively.

C-terminal region, where they contain the PH−BEACH−WD40 domains (Figure 1A and see below). Outside this region, there is generally little sequence homology among these proteins, consistent with their diverse cellular functions.

Nbea and LRBA/BGL are two BEACH proteins that share significant homology throughout their entire sequences and have homologues in *Drosophila* (AKAP550) (*17*) and *Caenorhabditis elegans*. Nbea may be involved in membrane traffic in neuronal cells (*9*). LRBA/BGL may have a function in polarized vesicle trafficking and is localized to vesicles after stimulation by lipopolysaccharide (LPS) (*10*). Several copies of truncated pseudogenes of LRBA/BGL are present in the human genome, one of which is located at the translocation breakpoint linked to B-cell lymphoma (*18*). The BEACH proteins of this subfamily contain a motif that binds the regulatory subunit of protein kinase A (Figure 1A), and such proteins are also known as A kinase-anchoring proteins (AKAPs) (*19*). Therefore, one function of these proteins may be to direct protein kinase A to selected locations in the cell. However, the AKAP motif contains only about 20 amino acid residues and therefore cannot account for the large size of these proteins (Figure 1A).

The WD40 domain is generally located at the extreme C terminus of these proteins (Figure 1A). It is more conserved at the structural level than at the sequence level and may be important for protein−protein interactions (*20*). The WD40 domain of FAN interacts with tumor necrosis factor receptor I (TNFRI) as well as CD40, thereby initiating signal transduction and apoptosis through these receptors (*12*, *21*). These effects are mediated by the activation of a neutral sphingomyelinase (*12*, *13*). The targets of the WD40 domains in other BEACH proteins are currently unknown.

The BEACH domain is located just prior to the WD40 domain in these proteins and is the only domain that is highly conserved among them (Figure 1B). The amino acid sequence identity between any pair of BEACH domains is generally 45% or higher, but this domain does not share any recognizable sequence homology with other proteins. The BEACH domain is crucial for the function of these proteins. Mutations found in CHS patients all give rise to the production of nonfunctional, truncated proteins that lack the BEACH and WD40 domains (*2*, *22*, *23*), suggesting the full-length CHS protein is required for its function. Recent studies in cell culture show that the WD40 domain of CHS has dominant negative effects, producing enlarged lysosomes that are reminiscent of the CHS disease (*24*).

The pleckstrin homology (PH) domain in these proteins was first identified from our structural studies of the BEACH domain region of Nbea (*25*). This PH domain is weakly conserved among the BEACH proteins and does not share

any recognizable sequence homology with other PH domains. This domain is intimately associated with the BEACH domain in the Nbea crystal structure (*25*). Studies with FAN suggest that the PH−BEACH−WD40 domains are required for its function (*25*), whereas the WD40 domain by itself has dominant negative effects (*12*).

Although a descriptive function for some of the BEACH proteins has been obtained, the molecular mechanism for their actions is currently unknown. For example, while the lack of functional CHS protein produces giant lysosomes, it is not known how the CHS protein contributes to the morphogenesis and/or trafficking of this organelle. Specifically, despite being the only domain that is highly conserved among these proteins, the exact molecular function of the BEACH domain is still not clear. We have recently reported the crystal structure of the PH−BEACH domains of Nbea (*25*). The structure shows that the BEACH domain has an unusual polypeptide backbone fold and that the BEACH domain has strong interactions with the novel PH domain. To further our understanding of these domains, we present here the crystal structure of the PH−BEACH domains of LRBA/BGL, as well as biophysical characterizations that confirm the high affinity between the PH and BEACH domains of FAN.

MATERIALS AND METHODS

Protein Expression and Purification. Residues 2073−2489 of the LRBA/BGL protein was subcloned into the pET28a vector (Novagen) and overexpressed in *E. coli* Star cells at 20 °C. The expression construct contains an N-terminal hexahistidine tag and covers the conserved BEACH domain together with the novel PH domain that we identified from our studies of neurobeachin (*25*). The soluble protein was bound to nickel-agarose affinity resin (Qiagen) and eluted with a buffer containing 20 mM Tris (pH 7.5), 250 mM NaCl, and 150 mM imidazole. The protein was further purified by anion-exchange chromatography at pH 7.5 and by gel-filtration chromatography in a running buffer containing 20 mM Tris (pH 7.5), 250 mM NaCl, and 10 mM DTT. The protein fractions from this column were pooled and concentrated to 25 mg/mL, flash-frozen in liquid nitrogen in the presence of 5% (v/v) glycerol, and stored at −80 °C. The N-terminal His-tag was not removed for crystallization.

Protein Crystallization. Crystals of the PH−BEACH domain of LRBA/BGL were obtained at 4 °C by the hanging-drop vapor-diffusion method. The reservoir solution contained 100 mM Hepes (pH 8.0), 0.2 M Mg formate, and 5−10% (v/v) glycerol. For cryo protection, 20% (v/v) ethylene glycol was introduced into the mother liquor, and the crystals were flash-frozen in liquid nitrogen for data collection at 100 K.

Data Collection. X-ray diffraction data to 2.4 Å resolution were collected on an ADSC Quantum-4 CCD at the X4A beamline of the National Synchrotron Light Source (NSLS). The diffraction images were processed and scaled with the HKL package (*26*). The data processing statistics are summarized in Table 1. The crystal belongs to the space group $P2_1$, with cell dimensions of $a = 73.2$ Å, $b = 102.2$ Å, $c = 131.5$ Å, and $\beta = 90.5°$. There are four molecules of the PH−BEACH domain in the asymmetric unit. As suggested by the β angle, the crystal has pseudo $P2_12_12_1$ symmetry. The R_{merge} for this higher symmetry is 11.7%, while that for $P2_1$ symmetry is 5.1% (Table 1), confirming that there is deviation from the $P2_12_12_1$ symmetry.

Table 1: Summary of Crystallographic Information

resolution range used in refinement (Å)	20−2.4
number of observations	167 893
R_{merge} (%)[a]	5.1 (15.9)
number of reflections	67 350
completeness (%)	89 (74)
R factor (%)[b]	21.0 (25.8)
free R factor (%)	25.8 (31.9)
rmsd in bond lengths (Å)	0.008
rmsd in bond angles (deg)	1.3
number of protein, solvent atoms	13 516, 494
average B values for protein, solvent atoms (Å^2)	38, 36

[a] $R_{merge} = \{\sum_h\sum_i|I_{hi} - \langle I_h\rangle|\}/\{\sum_h\sum_i I_{hi}\}$. The numbers in parenthesis are for the highest resolution shell. [b] $R = \{\sum_h|F_h^o - F_h^c|\}/\{\sum_h F_h^o\}$.

Structure Determination and Refinement. The initial structure of the PH−BEACH domain of LRBA/BGL was determined by the molecular replacement method, with the program COMO (*27*, *28*). The structure of the PH−BEACH domain of neurobeachin was used as the search model (*25*). The program automatically located all four copies of the molecule in the asymmetric unit. The atomic model was built into the electron density with the program O (*29*). The structure refinement was carried out with the program CNS (*30*). Noncrystallographic symmetry (NCS) restraints on the main-chain atoms were applied throughout the refinement. The statistics on the structure refinement are summarized in Table 1.

Biacore Studies. The PH domain of FAN (residues 183−298) was expressed and purified as a glutathione-*S*-transferase (GST) fusion protein, and the BEACH domain of FAN (residues 295−579) was expressed and purified as a His-tagged protein (*25*).

The surface plasmon resonance studies were carried out using a Biacore 3000 instrument (Biacore AB, Uppsala, Sweden). A monoclonal anti-GST antibody (Biacore AB) was immobilized on a CM5 biosensor chip using standard amine coupling. Control experiments showed that there was no binding of the BEACH domain to this antibody surface. GST−PH fusion protein was captured on the anti-GST surface at low (RU 550) and high (RU 1660) densities, using two of the available flow cells. To measure the kinetics and affinity of the interaction between the two domains, the BEACH domain was injected at concentrations from 890 to 11 nM using a 3-fold dilution series. The series was repeated 5 times over a period of 6 h to collect the response data.

Sensorgrams were processed to remove bulk refractive index changes and instrument drift using a reference surface. The equilibrium response data were fit to a single-site-binding model to extract affinities. The kinetic data from the low capacity surface were globally fit to a 1:1 binding model to determine the kinetics for complex formation and dissociation.

Fat Western Blotting Assay. The experiment was performed following protocols described earlier (*31*). A panel of phospholipids were purchased from Sigma and bound to nitrocellulose membranes. The PH domain of FAN (as the GST-fusion protein) and the PH−BEACH domain of Nbea (as His-tagged protein) were incubated with the membranes for 1 h at 4 °C. Bound protein was probed with anti-GST

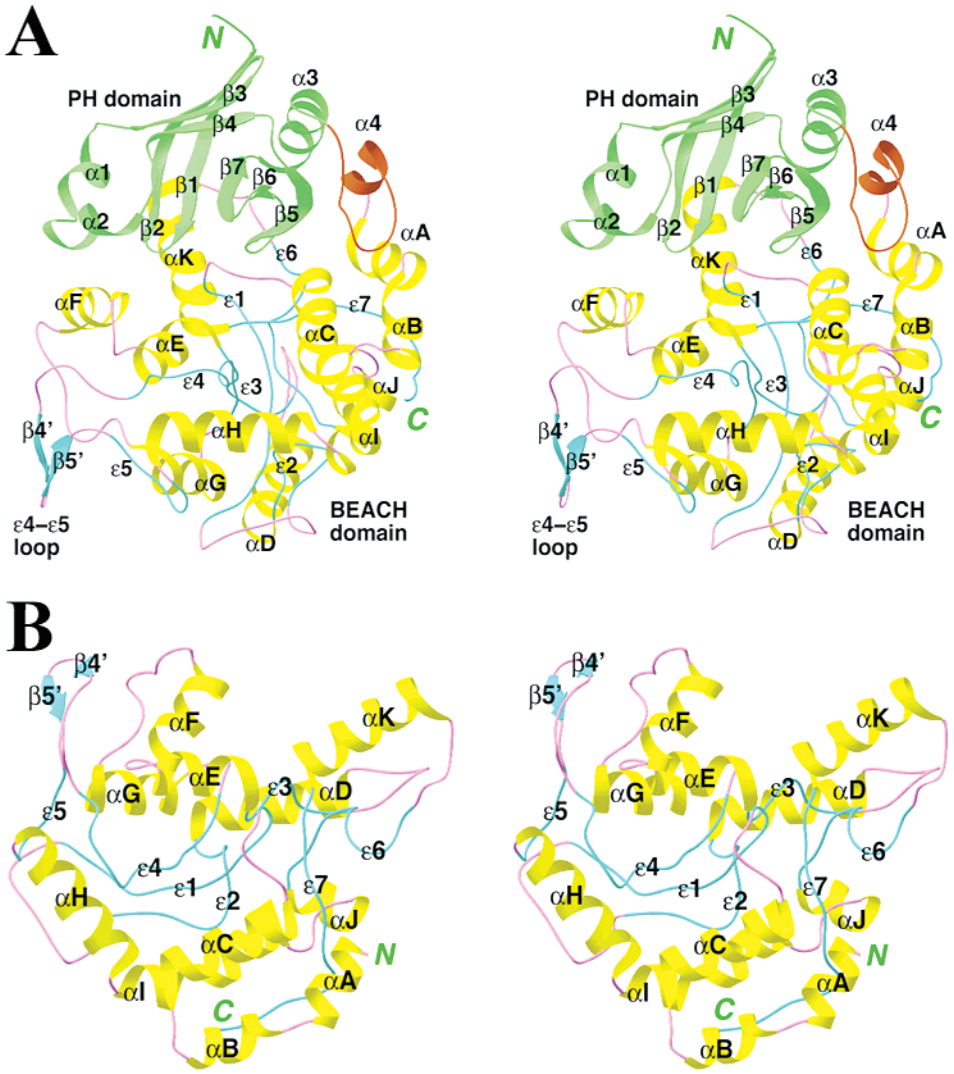

FIGURE 2: Structure of the PH−BEACH domains of LRBA/BGL. (A) Schematic drawing of the structure of the PH−BEACH domains of human LRBA/BGL. The PH domain is shown in green, and the linker is shown in orange. For the BEACH domain, the extended segments are shown in cyan; the α helices, in yellow; and the loops, in purple. (B) Schematic drawing of the structure of the BEACH domain of human LRBA/BGL. The view is related to that of A by roughly a 90° rotation around the horizontal axis, produced with ribbons (*34*).

and anti-His tag antibodies, respectively. As a positive control, the GST- and His-fusion proteins were detected with the antibodies using a regular Western protocol.

Atomic Coordinates. The atomic coordinates have been deposited in the Protein Data Bank, with the accession code 1T77.

RESULTS AND DISCUSSION

Structure Determination. The crystal structure of the PH−BEACH domains of human LRBA/BGL has been determined at 2.4 Å resolution (Figure 2A). The initial structure was determined by the molecular replacement method (*27*), using the structure of the PH−BEACH domain of human neurobeachin as the search model (*25*). The current atomic model contains residues 2076−2489 of the protein. The residues are numbered according to GenBank entry P50851 (10). The first three residues, together with the His tag at the N terminus, are disordered. The *R* factor for the structure is 21.0%. The crystallographic statistics are summarized in Table 1. Almost all of the residues (99.4%) are located in the most favored and additional allowed regions of the Ramachandran plot.

There are four molecules of the PH−BEACH domain in the asymmetric unit of the crystal. For ease of discussion, the molecules are named A, B, C, and D. Molecules C and D are related to molecules A and B by a pseudo-2_1 screw axis along the *c* axis of the unit cell, giving rise to the pseudo $P2_12_12_1$ symmetry for the crystal. The deviation from perfect crystallographic symmetry is fairly small, about 0.6° in orientation and 2 Å in position. This is consistent with our observation that the R_{merge} for the orthorhombic space group is only 11.7%. As a result of this pseudo symmetry, molecules A and B and C and D have essentially the same structure, with a root-mean-square (rms) distance of 0.25 Å for all of their equivalent Cα atoms. However, if molecule A is superimposed onto molecule C alone, the rms distance is only 0.13 Å, suggesting that there are small differences in the organization of the AB and CD dimers.

Molecules A and B are related by a noncrystallographic (NCS) 2-fold symmetry axis, which is oriented about 3° from

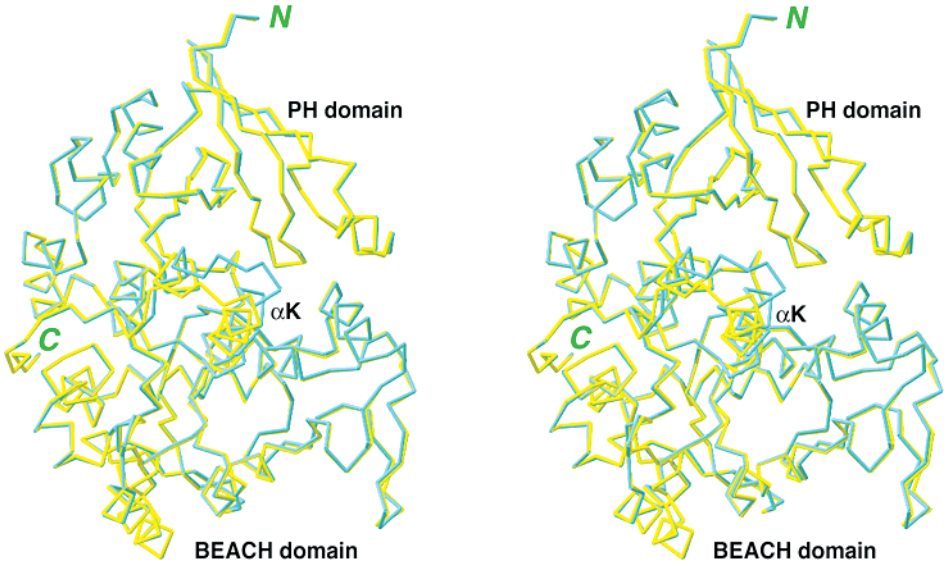

FIGURE 3: Structural differences between two PH−BEACH domain molecules of LRBA/BGL. The Cα traces of the two molecules are shown in yellow and cyan, respectively. The view is from the back of Figure 2A, to highlight the region of the largest difference near helix αK, produced with ribbons (*34*).

the unit cell *b* axis. The conformation of molecules A and B are also similar to each other, with a rms distance of 0.4 Å for 404 equivalent Cα atoms between them. Residues 2457−2466 (αK helix and the following loop in the BEACH domain) have large structural differences between the two molecules (Figure 3). They are involved in the contacts at the interface of this NCS dimer, which may be the reason for their conformational differences. The dimer interface is small, with 640 Å^2 of the surface area of each monomer buried, and more than half (390 Å^2) of the surface burial is due to residues 2457−2466. This suggests that the observed NCS dimer in the crystal is unlikely to be stable in solution, consistent with our light-scattering studies showing that this protein exists as monomers in solution.

Overall Structure. The PH domain covers residues 2076−2181 and contains a seven-stranded, antiparallel β sandwich (β1−β7) and an α helix (α3) near its C terminus (Figures 1B and 2A). This is the typical fold of canonical PH domains, although the PH domains of BEACH proteins share little sequence homology to these other PH domains. Another feature of the PH domain of LRBA/BGL is the presence of two small helices (α1 and α2) in the loop between strands β3 and β4 (Figure 2A), also observed in the structure of the PH−BEACH domains of Nbea (*25*). These helices partially block the binding site for phospholipid and phosphotyrosine in the other PH domains and suggest that the PH domain of LRBA/BGL may have a different function (see below) (*25*).

The BEACH domain covers residues 2200−2489 and contains 11 α helices (αA−αK) on the periphery of the structure (Figures 1B and 2A). As was observed in the structure of the BEACH domain of Nbea (*25*), the seven peptide segments (ϵ1−ϵ7) in the core of this domain are not fully extended (Figure 2A), and the main-chain atoms of these segments are mostly hydrogen-bonded to highly conserved side chains of the domain. The BEACH domain structure can be considered to have three layers, with the partially extended segments in the center of the structure flanked by helices on both sides (Figure 2B). Such a fold has not been seen in other protein structures. This novel backbone fold unfortunately makes it impossible to deduce the function of the BEACH domain based solely on the structural information.

The linker between the two domains is well-ordered and has intimate contacts with both domains (Figure 2A). The amino acid sequences of residues in this linker are poorly conserved among the various BEACH proteins (Figure 1B), but it is unlikely for this variation to affect the association between the PH and BEACH domains (see below) (*25*).

Comparison to the PH−BEACH Domains of Neurobeachin. The overall structure of the PH−BEACH domains of LRBA/BGL is similar to that of Nbea that we reported earlier (*25*), consistent with the 82% amino acid sequence identity shared by the two proteins (Figure 1B). A total of 275 of 290 Cα atoms can be superimposed between the BEACH domains of LRBA/BGL and Nbea, giving a rms distance of 0.54 Å (Figure 4).

Despite the high sequence homology, there are regions of significant structural differences between the two proteins. Residues 2376−2388 (ϵ4−ϵ5 loop) have the largest difference between the two structures (Figure 4). In the crystals of the PH−BEACH domains of Nbea, this loop is docked into the PH−BEACH interface of another molecule in the asymmetric unit (*25*) and therefore is located far from the rest of the BEACH domain (Figure 4). In comparison, this loop in molecules A and C contacts helix α3 of the PH domain from other molecules in the crystal of the PH−BEACH domains of LRBA/BGL, whereas this loop in molecules B and D are not involved in crystal packing. The loop is placed closer to the rest of the BEACH domain in the current structure (Figure 4), where it has interactions with the αF−αG loop (Figure 2A). Conformational differences are also seen for the αF helix and the αF−αG loop between the two structures (Figure 4). Two short antiparallel β strands (β4′ and β5′) are hydrogen-bonded to each other in the ϵ4−ϵ5 loop (Figure 2A). Overall, it is clear that this loop has significant inherent flexibility, which may be important for the biological functions of the BEACH domain.

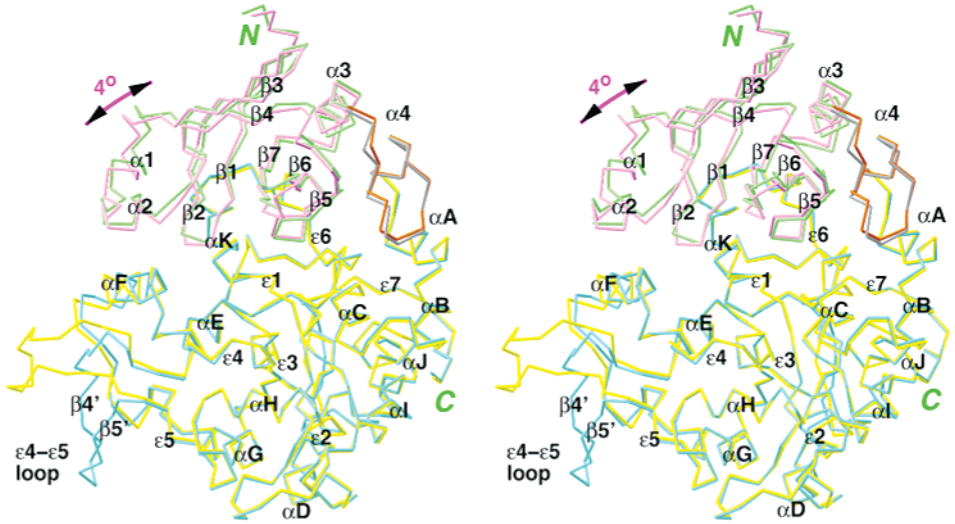

FIGURE 4: Structural differences between the PH−BEACH domains of LRBA/BGL and Nbea. The Cα traces of the PH, linker, and BEACH domains of LRBA/BGL are shown in green, gold, and cyan, respectively, and those of Nbea are shown in magenta, gray, and yellow, respectively. The region of the largest difference is in the $\epsilon 4-\epsilon 5$ loop. The rotation of 4° needed to bring the PH domains into overlap is also indicated, produced with ribbons (*34*).

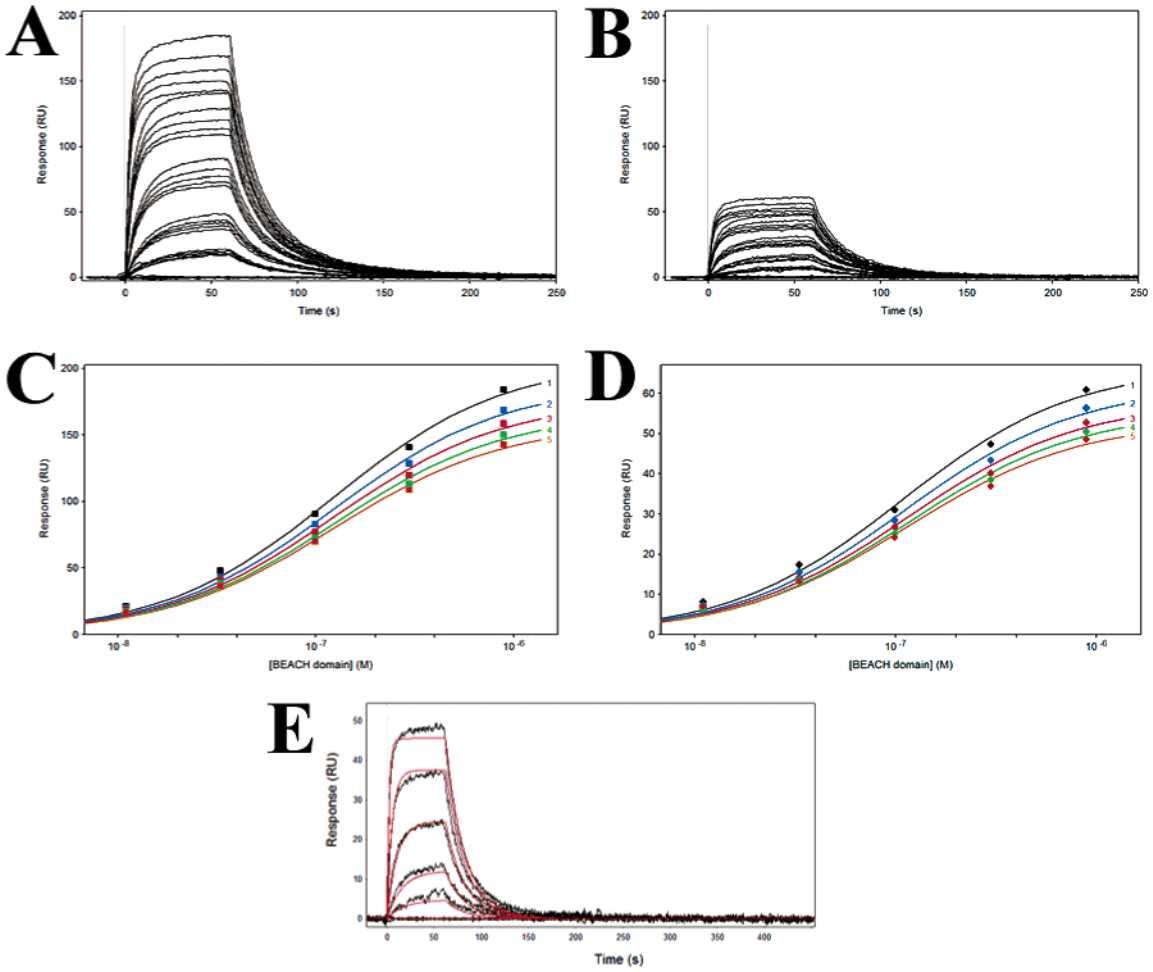

FIGURE 5: Characterization of PH−BEACH interactions by surface plasmon resonance. (A) Observed binding of the BEACH domain to the high-density GST−PH domain surface. (B) Observed binding of the BEACH domain to the low-density GST−PH domain surface. (C) Plot of the equilibrium binding response to the high-density GST−PH domain surface as a function of the BEACH domain concentration, for the five injection series. The curves represent a fit to the experimental data, assuming a 1:1 stoichiometry between the PH and BEACH domains. (D) Same as C but for the low-density GST−PH domain surface. (E) Fitting the observed binding data to the low-density GST−PH domain surface to extract the kinetic constants of the interactions. The predicted binding curves are shown in red.

With the BEACH domain in overlap, the PH domain of LRBA/BGL can be superimposed onto that of Nbea, giving a rms distance of 0.54 Å for 122 equivalent Cα atoms. This confirms that the PH domains of the two proteins share significant structural homology. However, this superposition requires a rotation of 4°, suggesting that there is a small

difference in the relative organization of the PH and BEACH domains between LRBA/BGL and Nbea (Figure 4).

Biacore Studies Show High Affinity between the PH and BEACH Domains. There is an extensive, highly conserved interface between the PH and BEACH domains in LRBA/BGL, similar to our original observations in Nbea (*25*). A total of about 1300 Å^2 of the surface area of the PH or BEACH domain is buried at this interface. One face of the β sheet in the PH domain (strands β1, β2, β5, β6, and β7) is docked over the surface of the BEACH domain (Figure 2A). The small rotation of the PH domain relative to the BEACH domain in LRBA/BGL has little impact on the interface between them. A consequence of the different packing interactions in the crystals of LRBA/BGL as compared to Nbea is that the PH−BEACH interface in the current structure is exposed to the solvent, in agreement with our earlier suggestion that the binding of the ϵ4−ϵ5 loop to the PH−BEACH interface in the Nbea structure is likely a crystallographic artifact (*25*).

On the basis of GST pull-down experiments, it was estimated that the affinity between the PH and BEACH domains of the protein FAN is about 1 μM (*25*). Moreover, mutations of residues in the PH−BEACH interface can disrupt the interaction between the two domains (*25*). We were not able to perform the binding assays with Nbea, because we cannot produce its PH domain as a soluble protein in bacteria. Nevertheless, the binding studies using the PH and BEACH domains of the homologous protein FAN are in good agreement with the extensive interactive interfaces between these domains, as revealed from the Nbea and LRBA/BGL crystal structures, and suggest that the intimate association between the PH and BEACH domains may be conserved in all of the BEACH proteins.

To obtain a more accurate measurement of the affinity between the two domains, we examined their interactions by surface plasmon resonance (*32*). A GST-fusion protein containing the PH domain of FAN was captured onto an anti-GST biosensor chip at two different densities, and the BEACH domain of FAN was injected over these surfaces. As expected, the observed binding responses were dependent on the concentration of injected BEACH domain (Figure 5A), as well as the density of the PH domain on the chip surface (Figure 5B). On the other hand, no binding of the BEACH domain was observed when the PH domain was not immobilized on the chip (data not shown), confirming the specificity of the interactions between the PH and BEACH domains.

To determine the K_d of the interaction, the responses at equilibrium are plotted versus the BEACH domain concentration for the high- and low-density PH domain surfaces. The observed binding curves can be nicely fit using a 1:1 interaction model (parts C and D of Figure 5), confirming the stoichiometry of the interaction between the PH and BEACH domains. On the basis of these data, the K_d value is determined to be 120 and 110 nM, for the high- and low-density PH domain surfaces, respectively (Table 2), showing excellent agreement between the measurements from the two surfaces. There was a small decrease (about 7%) in the binding response when the BEACH domain was re-injected over the PH domain chip surface (parts C and D of Figure 5), but the K_d of the interaction did not change (Table 2). This decrease in response is likely due to the loss of activity (for example, unfolding) of either the PH or BEACH domain during the time of the experiment. This is not unexpected when reactions are studied over a period of 6 h. Overall, the biosensor data demonstrate that there are strong interactions between the PH and BEACH domains. The data validate our earlier estimated K_d value of 1 μM based on GST pull-down experiments (*25*) and are consistent with the extensive interface between the two domains as observed in our structures.

To obtain estimates of the binding kinetics between the PH and BEACH domains, the experimental data from the lower capacity PH domain surface are globally fit to a 1:1 interaction model to extract the kinetic constants (Figure 5E). The rate of association (k_a) is 4.6 × 10^5 M^{-1} s^{-1}, and the rate of dissociation (k_d) is 0.49 s^{-1}. These are fairly typical binding constants for protein−protein interactions, indicating the association is specific and complex formation is fully reversible.

Table 2: Affinity between the PH and BEACH Domains of FAN

	high-density PH domain surface		low-density PH domain surface	
injection series	K_d (nM)	response unit	K_d (nM)	response unit
1	122 ± 2	206 ± 1	107 ± 3	67 ± 0.5
2	123 ± 3	189 ± 1	112 ± 3	62 ± 0.5
3	124 ± 3	177 ± 1	114 ± 3	58 ± 0.5
4	125 ± 3	168 ± 1	116 ± 3	56 ± 0.5
5	123 ± 3	160 ± 1	113 ± 4	53 ± 0.5

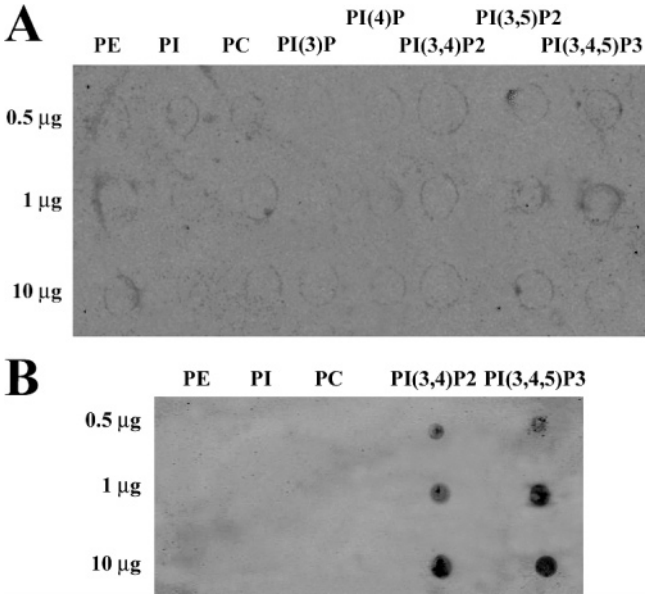

FIGURE 6: Characterization of phospholipid binding. (A) Phospholipid binding by the PH−BEACH domains of LRBA/BGL. Increasing amounts of various phospholipids were spotted on a nitrocellulose membrane. After incubation with the PH−BEACH domains of LRBA/BGL as a His-tagged protein, the bound protein was probed with an anti His-tag antibody. The lack of response suggests no detectable binding of the PH−BEACH domains to any of the phospholipids tested. PE, phosphatidylethanolamine; PI, phosphatidylinositol; PC, phosphatidylcholine; PI(3)P, phosphatidylinositol 3-monophosphate; PI(4)P, phosphatidylinositol 4-monophosphate; PI(3,4)P2, phosphatidylinositol 3,4-bisphosphate; PI(3,5)P2, phosphatidylinositol 3,5-bisphosphate; PI(3,4,5)P3, phosphatidylinositol 3,4,5-trisphosphate. (B) Phospholipid binding by the PH domain of Grp1 (*33*). Clear evidence for binding was observed for the PI(3,4)P2 and PI(3,4,5)P3 phospholipids.

PH Domain in BEACH Proteins Cannot Bind Phospholipids. Our structural studies on the BEACH proteins revealed a novel PH domain. However, detailed structural analyses suggest that this PH domain is unlikely to bind phospholipids, because the binding site is blocked by helix α2 in the structure, a unique feature of the PH domains from Nbea and LRBA/BGL. In addition, the surfaces of these PH domains do not have the clustering of positively charged side chains that may be important for binding the highly negatively charged phospholipids (*25*).

To experimentally assess the capability of the PH and PH−BEACH domains to bind phospholipids, we performed dot-blot binding assays using a panel of different phospholipids. The PH−BEACH domains of LRBA/BGL did not bind any of the tested phospholipids in these assays (Figure 6A), supporting the prediction of the structural analyses. Similarly, no binding was detected with the PH−BEACH domains of Nbea or the PH domain of FAN (data not shown). As a positive control, we have expressed and purified the PH domain of Grp1, following protocols described earlier (*33*). The dot-blot assay clearly showed binding to phospholipids by this PH domain (Figure 6B), consistent with earlier results (*33*) and validating our dot-blot assay.

The large sizes of the BEACH proteins and their unique amino acid sequences have severely hindered the elucidation of the functions of these proteins and their domains. We have determined the crystal structure of the PH−BEACH domains of human LRBA/BGL and demonstrated the strong affinity between the PH and BEACH domains of the protein FAN by surface plasmon resonance measurements. The structural and biophysical information provides a molecular basis for understanding the cellular functions of these domains once they become available.

ACKNOWLEDGMENT

We thank Reza Khayat, Hailong Zhang, and Javed Khan for help with the data collection at the synchrotron and structure refinement; Randy Abramowitz and Craig Ogata for setting up the beamline at NSLS; Dixie Mager for providing the human BGL cDNA; and William Kerr for providing the murine LRBA cDNA.

REFERENCES

1. de Lozanne, A. (2003) *Traffic 4*, 6−12.
2. Introne, W., Boissy, R. E., and Gahl, W. A. (1999) *Mol. Gen. Metab. 68*, 283−303.
3. Spritz, R. A. (1998) *J. Clin. Immunol. 18*, 97−105.
4. Ward, D. M., Griffiths, G. M., Stinchcombe, J. C., and Kaplan, J. (2000) *Traffic 1*, 816−822.
5. Dell'Angelica, E. C., Mullins, C., Caplan, S., and Bonifacino, J. S. (2000) *FASEB J. 14*, 1265−1278.
6. Nagle, D. L., Karim, M. A., Woolf, E. A., Holmgren, L., Bork, P., Misumi, D. J., McGrail, S. H., Dussault, J., B. J., Perou, C. M., Boissy, R. E., Duyk, G. M., Spritz, R. A., and Moore, K. J. (1996) *Nature Gen. 14*, 307−311.
7. Perou, C. M., Moore, K. J., Nagle, D. L., Misumi, D. J., Woolf, E. A., McGrail, S. H., Holmgren, L., Brody, T. H., Dussault, J., B. J., Monroe, C. A., Duyk, G. M., Pryor, R. J., Li, L., Justice, M. J., and Kaplan, J. (1996) *Nature Gen. 13*, 303−308.
8. Barbosa, M. D. F. S., Nguyen, Q. A., Tchernev, V. T., Ashley, J. A., Detter, J. C., Blaydes, S. M., Brandt, S. J., Chota, D., Hodgman, C., Solari, R. C. E., Lovett, M., and Kingsmore, S. F. (1996) *Nature 382*, 262−265.
9. Wang, X., Herberg, F. W., Laue, M. M., Wullner, C., Hu, B., Petrasch-Parwez, E., and Kilimann, M. W. (2000) *J. Neurosci. 20*, 8551−8565.
10. Wang, J.-W., Howson, J., Haller, E., and Ker, W. G. (2001) *J. Immunol. 166*, 4586−4595.
11. Feuchter, A. E., Freeman, J. D., and Mager, D. L. (1992) *Genomics 13*, 1237−1246.
12. Adam-Klages, S., Adam, D., Wiegmann, K., Struve, S., Kolanus, W., Schneider-Mergener, J., and Kronke, M. (1996) *Cell 86*, 937−947.
13. Kreder, D., Krut, O., Adam-Klages, S., Wiegmann, K., Scherer, G., Plitz, T., Jensen, J.-M., Proksch, E., Steinmann, J., Pfeffer, K., and Kronke, M. (1999) *EMBO J. 18*, 2472−2479.
14. Nagase, T., Kikuno, R., Nakayama, M., Hirosawa, M., and Ohara, O. (2000) *DNA Res. 7*, 273−281.
15. Kwak, E., Gerald, N., Larochelle, D. A., Vithalani, K. K., Niswonger, M. L., Maready, M., and de Lozanne, A. (1999) *Mol. Biol. Cell 10*, 4429−4439.
16. Cornillon, S., Dubois, A., Bruckert, F., Lefkir, Y., Marchetti, A., Benghezal, M., de Lozanne, A., Letourneur, F., and Cosson, P. (2002) *J. Cell Sci. 115*, 737−744.
17. Han, J.-D., Baker, N. E., and Rubin, C. S. (1997) *J. Biol. Chem. 272*, 26611−26619.
18. Dyomin, V. G., Chaganti, S. R., Dyomina, K., Palanisamy, N., Murty, V. V. V. S., Dalla-Favera, R., and Chaganti, R. S. K. (2002) *Genomics 80*, 158−165.
19. Colledge, M., and Scott, J. D. (1999) *Trends Cell Biol. 9*, 216−221.
20. Neer, E. J., Schmidt, C. J., Narabudripad, R., and Smith, T. F. (1994) *Nature 371*, 297−300.
21. Segui, B., Andrieu-Abadie, N., Adam-Klages, S., Meilhac, O., Kreder, D., Garcia, V., Bruno, A. P., Jaffrezou, J.-P., Salvayre, R., Kronke, M., and Levade, T. (1999) *J. Biol. Chem. 274*, 37251−37258.
22. Certain, S., Barrat, F., Pastural, E., le Deist, F., Goyo-Rivas, J., Jabado, N., Benkerrou, M., Seger, R., Vilmer, E., Beullier, G., Schwarz, K., Fischer, A., and de Saint Basile, G. (2000) *Blood 95*, 979−983.
23. Karim, M. A., Nagle, D. L., Kandil, H. H., Burger, J., Moore, K. J., and Spritz, R. A. (1997) *Human Mol. Gen. 6*, 1087−1089.
24. Ward, D. M., Shiflett, S. L., Huynh, D., Vaughn, M. B., Prestwich, G., and Kaplan, J. (2003) *Traffic 4*, 403−415.
25. Jogl, G., Shen, Y., Gebauer, D., Li, J., Wiegmann, K., Kashkar, H., Kronke, M., and Tong, L. (2002) *EMBO J. 21*, 4785−4795.
26. Otwinowski, Z., and Minor, W. (1997) *Method Enzymol. 276*, 307−326.
27. Jogl, G., Tao, X., Xu, Y., and Tong, L. (2001) *Acta Crystallogr., Sect. D 57*, 1127−1134.
28. Tong, L. (1996) *Acta Crystallogr., Sect. A 52*, 782−784.
29. Jones, T. A., Zou, J. Y., Cowan, S. W., and Kjeldgaard, M. (1991) *Acta Crystallogr., Sect. A 47*, 110−119.
30. Brunger, A. T., Adams, P. D., Clore, G. M., DeLano, W. L., Gros, P., Grosse-Kunstleve, R. W., Jiang, J.-S., Kuszewski, J., Nilges, M., Pannu, N. S., Read, R. J., Rice, L. M., Simonson, T., and Warren, G. L. (1998) *Acta Crystallogr., Sect. D 54*, 905−921.
31. Stevenson, J. M., Perera, I. Y., and Boss, W. F. (1998) *J. Biol. Chem. 273*, 22761−22767.
32. Myszka, D. G. (2000) *Methods Enzymol. 323*, 177−207.
33. Ferguson, K. M., Kavran, J. M., Sankaran, V. G., Fournier, E., Isakoff, S. J., Skolnik, E. Y., and Lemmon, M. A. (2000) *Mol. Cell 6*, 373−384.
34. Carson, M. (1987) *J. Mol. Graphics 5*, 103−106.

BI049498Y